Astron. Astrophys. 354, 315–320 (2000)

ASTRONOMY AND ASTROPHYSICS

Speckle interferometry measurements of the asteroids 10–Hygiea and 15–Eunomia

R. Ragazzoni[1], **A. Baruffolo**[1], **E. Marchetti**[2], **A. Ghedina**[2], **J. Farinato**[3], **and T. Niero**[4]

[1] Astronomical Observatory of Padova, Vicolo dell'Osservatorio 5, 35122 Padova, Italy
[2] Centro Galileo Galilei, Apartado 565, 38700 Santa Cruz de la Palma, Spain
[3] European Southern Observatory, Karl-Schwarzschild-Strasse 2, 85386 Garching bei München, Germany
[4] Stazione Astronomica di Cagliari, Loc. Poggio dei Pini, Strada 54, 09012 Capoterra, Italy

Received 1 June 1999 / Accepted 19 November 1999

Abstract. Speckle interferometry measurements of the asteroids 10–Hygiea and 15–Eunomia have been obtained with the speckle facility aboard the AdOpt@TNG module, permanently mounted on the 3.58m TNG telescope in Canary Islands. Direct angular diameter measurements and estimates of the apparent ellipticity are given allowing to derive the density of these asteroids, combining our data with published results. Our data for 15–Eunomia, moreover, are compatible with both an egg–shaped and a double, in contact, asteroid model. A brief discussion of both models is here presented.

Key words: methods: data analysis – techniques: interferometric – minor planets, asteroids

1. Introduction

Asteroids exhibit size that are essentially below seeing limited capabilities of direct, ground based, angular diameter measurements even under the most exceptional seeing conditions (maybe with the exceptions of very few, and already well studied, large asteroids). On the opposite several asteroids can exhibit angular diameters larger than the diffraction limit of a 4m class telescope and hence can be at least measured in their angular size by speckle interferometry (Labeyrie 1970). From the inspection of the diameter tables published by Tedesco (1989) and of the orbital semimajor axis a published by Williams (1989) one can see that, at a distance of $a - 1$ AU, experienced in an *average* opposition, and assuming an observing wavelength of $\lambda = 500$nm for a $D = 3.58$m telescope, among the first 200 numbered asteroids only 26 fall below the diffraction limit. This means that, including also the several Near–Earth Objects, at least a few hundreds asteroids can become targets for a speckle facility like the one implemented inside the AdOpt@TNG module (Ragazzoni & Bonaccini 1995; Ragazzoni et al. 1998), an adaptive optics instrument aboard the TNG telescope (Barbieri 1997; Bortoletto et al. 1998). Currently, few asteroids have reliable diameter measurements independently from any albedo assumption (although, as we show in the following, speckle measurements can still slightly depend upon some assumptions on the reflectance characteristics of the asteroid's surfaces).

The main interest in the determination of the absolute dimension of these objects (lightcurve fitting allowing reasonable estimates of the shape, Barucci et al. 1992) consists in the possibility to calculate their density and hence to give hints on their physical nature. Mass measurements by asteroid scattering (Hilton et al. 1996) allow to obtain estimates with precisions rarely better than 10% (sometimes only upper limits can be placed). We do not consider here *in situ* measurements by means of spacecraft because in these cases diameter and shape determinations from the ground are hopelessly irrelevant with respect to the spacecraft data. In order to obtain volume data of comparable quality one needs to have reliable and albedo–independent measurements with precisions of the order of 5%. This is not a simple task for speckle interferometry and care is to be taken in the data collection and analysis to ensure such a result.

Of course, a program for asteroid accurate size measurement should be limited to the asteroids that have some chances to get a reliable determination of the mass. Kuzmanoski & Knezevic (1993) provided a list of 208 close pair encounters useful for mass measurements, involving 115 different scattering asteroids. Their analysis has been performed selecting the largest asteroids so that it is reasonable that most of them will exhibit angular sizes larger than the diffraction limit. In conclusion, such a crude selection leads to at least one hundred asteroids suitable for a measurement program. In contrast less than ten asteroids have been measured up to now by speckle interferometry (Angel 1977; Baier & Weigelt 1983; Drummond et al. 1985ab; Worden et al. 1977; Worden & Stein 1979). Rotation of the asteroids and different Sun–asteroid–Earth phase angles introduce the possibility to constrain a model for the asteroid even further. These approaches have been developed especially in conjunction with lightcurve photometric analysis leading to very interesting results, although limited to a few cases (Drummond & Hege 1986). More detailed analysis of specklegrams can lead to a full recovery of the image of the observed asteroid (Drummond et al. 1988). In our speckle facility this last

Send offprint requests to: R. Ragazzoni

Table 1. Observation circumstances and literature data relevant to the discussion in the text. Notes: (1) add 2451000; (2) from JPL/Horizon ephemerides; (3) the scales along two axes of detector differs of $\approx 8\%$ and here are reported the average values; (4) epoch and period are from Michalowski et al. (1991); (5) epoch is from Scaltriti & Zappalá (1975), while we adopted the revised period given by Magnusson (1986); both phases are tuned in order to give zero at maxima; (6) Tholen (1989); (7) Tedesco (1989); (8) Scholl et al. (1987); (9) Hilton (1997); (10) we used $M_\odot = 1.9891 \cdot 10^{30}$kg; (11) assuming homogeneous density and a purely spherical shape.

	10–Hygiea	15–Eunomia
Date	Dec. 17, 1998	Dec. 17, 1998
Time (UT)	$5^h48^m30^s$	$0^h10^m7^s$
Julian Day (1)	164.7417	164.507
V mag. (2)	11.0	8.5
Δ [AU] (2)	2.67	1.70
Scale [km/px] (3)	≈ 48.2	≈ 30.7
Exp. time [sec.]	600	250
Filter ($\lambda/\Delta\lambda$) [nm]	580/100	580/100
STF star	HD 89112	HD 14155
Phase Angle (2)	16.7°	18.4°
Rotational phase	0.636 (4)	0.119 (5)
Barucci class (6)	C0	S0
IRAS diameter [km] (7)	429 ± 8	272 ± 6
Mass [$M_\odot \cdot 10^{-12}$]	47 ± 23 (8)	4.2 ± 1.1 (9)
Mass [10^{18}kg] (10)	93 ± 56	8.35 ± 2.19
Density [10^3kg/m^3] (11)	2.3 ± 1.5	0.80 ± 0.26

option is not possible, however data reduction is greatly simplified because real–time power spectrum is available at the end of the exposure. Speckle data collection of relatively bright asteroids requires a limited amount of time and could be efficiently performed in service–observing mode for a telescope equipped with an on–line speckle facility.

Here we present preliminary results with this instrument. Other types of speckle measurements, performed in this very early stage of instrument commissioning, are reported elsewhere (Ragazzoni et al. 2000).

2. Observations

The collected data consist of the accumulated power spectrum of the specklegrams of the asteroid and of a nearby star used as calibrator, also said STF (Speckle Transfer Function). The observer can work on a manageable amount of data whose reduction can be obtained in an almost automatic manner. On the other hand the drawback is that individual speckle frames are lost in our system and any further attempt to recover the phase of the Fourier spectra is impossible. A detailed description of the speckle facility can be found in Marchetti et al. (1997) and Mallucci (1998) while the real–time data acquisition is described in detail in Baruffolo, Ragazzoni & Farinato (1998).

During the commissioning phase of the AdOpt@TNG module (December 16th and 17th, 1999), we tested the speckle channel. All the measurements described here refer to the second night. Observations have been made under a poor seeing of ≈ 1.5arcsec for 10–Hygiea and of ≈ 2arcsec for 15–Eunomia. Scale calibration has been performed through observation of subarcsecond double stars leading to a scale of ≈ 0.025 arcsec per pixel. During our run the derotating system was not activated and some field rotation was experienced in the exposures. This amounts to less than 3 degrees in both cases and they are neglected here. Position angles given here refer to the average parallactic angle during the exposures. Speckle frames have been collected with 20mSec. single exposure time. All of the most relevant parameters for the observation discussed here are reported in Table 1 together with some literature–based data useful for the following discussion.

3. Reduction process

After the careful removing of the photon bias (Drummond & Hege 1989; Christou 1988; Pehlemann et al. 1992; Thiébaut 1994), the power spectra of the asteroid has been normalized using the STF power spectrum. We have made extensive tests changing the average number of photons assumed per each specklegram, in order to examine the results with respect to different assumptions on the photon bias correction. We have found small differences (less than 2%) in the final diameter measurements. We have made the initial choice to exploit data reduction directly in the Fourier space rather than in the autocorrelograms. We have selected the central portion of the power spectrum, corresponding to spatial frequencies in the range equivalent to sizes smaller than the diffraction limited capabilities of the telescope. The support of the spectra has been modelled by a quadratic term, while the asteroid signal has been modelled by a Gaussian shape. In practice, we have divided each power spectra into N_θ 'X'–shaped strips centered on the origin of the power spectra and encompassing a position angle interval $\Delta\theta$ where we have fitted the following relationship:

$$W(\rho) = a_0 + a_1\rho^2 + a_2 \exp\left(-\frac{\rho^2}{2a_3^2}\right) \quad (1)$$

where ρ is the distance from the power spectrum origin and $a_0 \ldots a_3$ are left as free parameters for the best fit operation.

After performing this curve fitting for several position angles θ, we obtain the function $a_3(\theta)$ that gives an estimate of the size of the power spectrum along a given position angle. Because of the central symmetry in the squared power spectrum we have performed N_θ measurements, spaced in the $0 \ldots 180$ degree interval, and using an angle interval $\Delta\theta$ usually larger than $180^\circ/N_\theta$, in order to improve the SNR with little expense of the angular sampling (this approach is equivalent to a smoothing in the $a_3(\theta)$ function with a boxcar of size $N_\theta\Delta\theta/180^\circ$). For each fitting, a formal error for the coefficient is obtained. We have normally used $N_\theta = 9$ and $\Delta\theta = 30^\circ$. The angular size of the asteroid is proportional to the $a_3^{-1}(\theta)$, but a careful calibration must be performed, as discussed below.

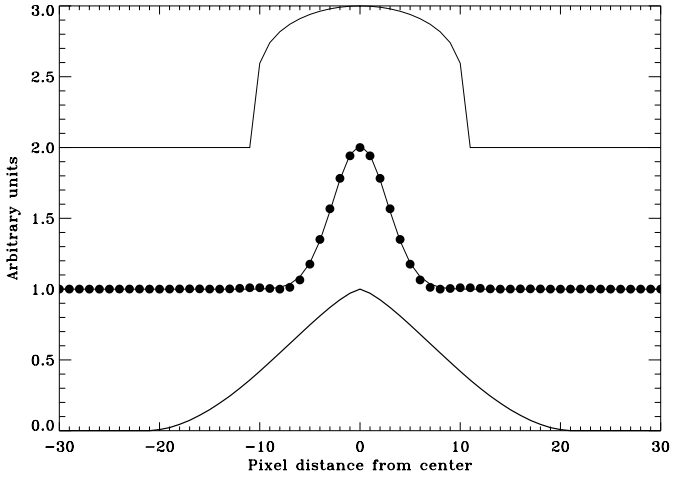

Fig. 1. The profiles for a Minnaert model with $k = 0.60$ (upper); the profile of the bidimensional Fourier transform (filled circles) fitted by a Gaussian function (middle) and the profile of the autocorrelation of the used model (bottom). For clarity the various curves have been displaced between each other.

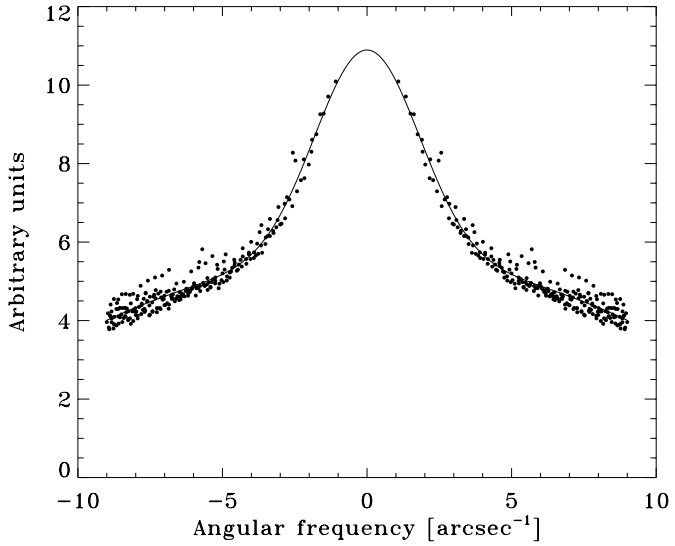

Fig. 2. Fit to a power spectrum profile for 10–Hygiea. Note the symmetry around the null angular frequency, due to the phase–lacking speckle interferometry technique here adopted.

3.1. The case for 10–Hygiea

Following Albrecht et al. (1994), we have assumed that the light distribution across the resolved disk of the asteroid follows a Minnaert law (Minnaert, 1941), given by:

$$I(\psi) = \cos^{2k-1}\psi, \tag{2}$$

where ψ is the angle between the normal to the surface and the observer line of sight.

This light distribution is much simpler than the detailed law given by Hapke (1984) but in several cases the difference may be small (McEwen 1991). We have generated several simulated light distributions (sampled with our detector scale), for instance, with different diameters and k; after performing the square Fourier transformation, we have fitted it with a Gaussian using the same code used to fit the observational data. Although in Fig. 1 linear traces are shown, all the calibration has been performed bidimensionally with circular objects. In this way one can calibrate the real diameter of the object with respect to the fitted a_3 coefficient. We have found a little dependence upon the choice for k. We have used $k = 0.60$ and we refer to the final discussion for the effects of a different Minnaert constant. Once the final estimate of the size of the asteroid has been obtained in the form of a function $r(\theta)$ with corresponding formal errors $\sigma_r(\theta)$ we have evaluated an average diameter d weighting the single measurements by $1/\sigma_r(\theta)$.

Table 2. The final estimated values for 10–Hygiea.

10–Hygiea	
Average diameter [km]	444 ± 35
Ellipticity a/b	1.11
Position angle ϕ	175°
Density [$10^3 kg/\mathrm{m}^3$]	2.0 ± 1.6

In order to have a reliable estimate of the diameter error, we have performed the calculation for several pairs of N_θ and $\Delta\theta$, averaging the final values and computing their standard deviation. The related figures are reported in Table 2, a sample fit to a power spectrum profile is shown in Fig. 2.

In order to estimate further shape features we have calculated the first coefficient of the discrete Fourier transform for the radial profile. In practice, we have fitted a function given by:

$$\rho(\theta) = d/2 + c\sin(2\theta + \phi). \tag{3}$$

From c, one can estimate the ratio of the apparent major axis with respect to the minor one, a/b, given by:

$$\frac{a}{b} = \frac{d + 2c}{d - 2c}. \tag{4}$$

We do not report, however, any error in the coefficient c, for the corresponding axis ratio a/b, and for the position angle ϕ. It is worth noting that the latter contains a 180° ambiguity, as in any phase–lacking speckle measurement.

3.2. The case for 15–Eunomia

The fitting in the Fourier space, in the case of 15–Eunomia, turned out to be more difficult than for 10–Hygiea. We interpret this fact as a consequence of the rather complicated shape of the measured object autocorrelation. In order to rule out possible ambiguities in the interpretation, we thus preferred to perform model fitting directly in the autocorrelation space rather than in the Fourier one (see Fig. 3).

From the fitting, and assuming a simple spherical shape for the asteroid, we derive a mean diameter of 305 ± 22km; this translates in a volume 30% larger than inferred from IRAS data. By combining this with the published mass estimate (Hilton 1997) we obtain an unrealistically small density of $0.56 \pm 0.27 \times 10^3$ kg $\cdot$ m^{-3}.

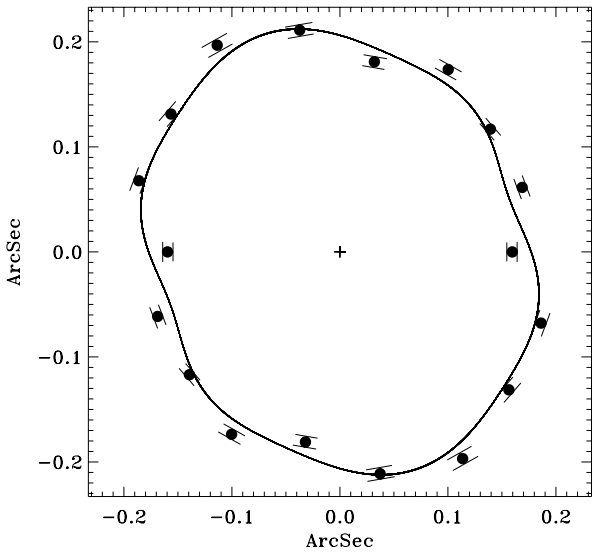

Fig. 3. Autocorrelation of 15–Eunomia, error bars are the formal standard deviation to the fit of the power spectrum strip. The fit has been performed using Eq. (3) with the addition of a $\sin(6\theta)$ term, in order to better model its hexagonal shape.

Although a bias in the mass measurement can explain our result, we found of some interest to investigate other models for the shape of 15–Eunomia, besides the simple, spherical, one.

In generating our models we did not take into consideration the variations of albedo over the asteroid's surface, although they are known to exist (Reed et al. 1997). However, given the intrinsic limits of our obervational technique, which does not allow to retrieve the phase of the Fourier spectra, we did not want to introduce too many degrees of freedom in our models, which would not have been sufficiently constrained by our data.

From Fig. 3 it can be seen that the 15-Eunomia autocorrelogram exhibits an hexagonal shape, suggesting a strong non-sphericity for this object. We thus modelled the asteroid's shape with an egg–like profile given by the following cartesian coordinates:

$$\begin{cases} x = a\,(2\cos\theta + \eta\cos 2\theta) \\ y = b\,(2\sin\theta - 2\eta\sin 2\theta) \end{cases} \tag{5}$$

where the coefficient η gives the *roundness* of the edges while a and b are proportional to the model sizes. We adopted here $\eta = 0.2$. In Fig. 4 a synthetic image generated according to Eq. (5) and its autocorrelation function is shown. The autocorrelogram exhibits an hexagonal shape, consistently with our measurements (Fig. 3).

From this model we derive a major and minor axis of 370 ± 39km and 240 ± 20km, respectively, and an asteroid's density of $1.04 \pm 0.57 \times 10^3$ kg $\cdot$ m^{-3}, which is still a somewhat low value. We thus continued our investigation by considering a two–components model for 15–Eunomia.

In fact our data are *consistent* with a binary asteroid model; see also Cellino et al. (1985) for a discussion about the lightcurve. This allows for an independent mass measurement which could potentially lead to a more reasonable density estimate.

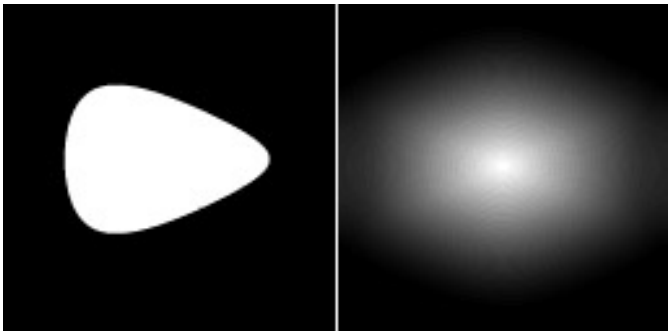

Fig. 4. A synthetic image of 15–Eunomia, generated using the *egg-like* model described in the text, and its autocorrelation function of hexagonal shape. Here the light distribution has been considered uniform on the whole cross–section, corresponding to $k = 0.5$.

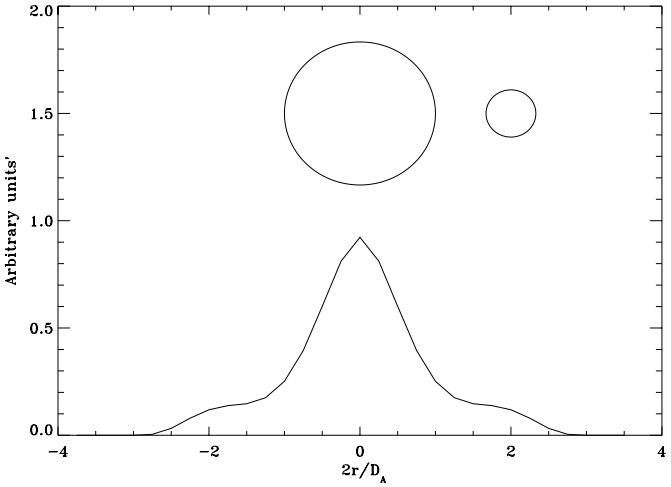

Fig. 5. The ACF of a very close double asteroid (sketched above the graph) could not exhibit secondary peaks. In this case the distance between the two components is equal to the diameter of the main one. The diameter ratio is $\gamma = 0.33$. This model uses $k = 0.6$.

We tentatively modelled the asteroid as an object made up of two components, A and B, of spherical shape, with $D_A > D_B$ the corresponding diameters, and r the distance of their mass centers. With respect to an ovoidal elongated shape, this model shows higher density for a given overall size. It is interesting to point out that the ACF of a binary asteroid does not exhibit a secondary peak when r is comparable to (or less than) D_A. In Fig. 5 the behaviour of the ACF trace of a binary asteroid with $D_A/r = 1$ is sketched. Negative results for the duplicity of 15–Eunomia by other speckle observations (Roberts et al. 1995) could be explained in this perspective. Moverover, under this condition, only the observations performed around the maximum of lightcurve (as in our case) can reveal the duplicity, in other cases being the projected cross–section of the double asteroid undistinguishable from a single object.

The position angle of the observed pair is $60^\circ \pm 15^\circ$ in good agreement with the position angle for the major axis of

Table 3. The final estimated values for the two models of 15–Eunomia. Notes: (1) the average diameters of the two component is given; (2) the ratio is the one of the envelope of the doublet; (3) using Keplerian mass estimate.

15–Eunomia	Egg–shaped	Double
Sizes [km]	370 ± 39	240 ± 20 (1)
	240 ± 20	60 ± 17
Ellipticity a/b	≈ 1.4	1.54 ± 0.28 (2)
Position angle ϕ_2	$60^\circ \pm 15^\circ$	
Density [$10^3 \mathrm{kg/m^3}$]	1.04 ± 0.57	1.79 ± 0.95(3)

the single object model of 15–Eunomia (from Bureau des Longitudes service). From the fitting of the autocorrelogram at an orthogonal position angle we have found our best estimate of $D_A = 240 \pm 20$km.

We have computed a grid of 11×11 models with 15–Eunomia A and B having the same albedo and with $D_B/D_A = \gamma$, varying in the range from 0.20 to 0.70 (corresponding to D_B ranging from 48km to 168km) and r ranging from 150 to 250km with steps of 0.05 and 10km respectively, and comparing them with the observations. We found a maximum likelihood with our measurements for $\gamma = 0.25 \pm 0.05$ (corresponding to $D_B = 60 \pm 17$ km) and $r = 220 \pm 20$km. The density becomes now $\rho = (1.14 \pm 0.59) \times 10^3 \mathrm{kg \cdot m^{-3}}$.

Being $(D_A^2 + D_B^2)/D_{\mathrm{IRAS}}^2 = 0.83 \pm 0.12$, the overall cross–section for our model is marginally smaller than the IRAS one.

In Fig. 6 our ACF measurements and the corresponding profiles computed from the model are shown. A few comments are needed in order to discuss these results. Because of the noisy background in the ACF image, which especially interests the smaller signature of the possible B component, it is possible that its size is underestimated. The overall size of the asteroid $(D_A + D_B)/2 + r = 370 \pm 39$km should not be affected by this problem.

This means that, although formally the spacing between 15–Eunomia A and B is 78 ± 47km, we cannot rule out the possibility that the two asteroid components are in contact.

Using Kepler's third law, the binary model gives a period estimate of $P = 7.63^h \pm 2.02^h$ consistent with the observed one (Scaltriti & Zappalá 1975) of $P = 6.08^h$; this last figure is affected by an extremely low relative error with respect to any other measurement reported here.

By inverse reasoning, we are now in a position to perform an independent estimate of the dynamic mass of the whole 15–Eunomia system using our r measure and lightcurve period P: we find a mass value $M = (1.32 \pm 0.36) \times 10^{19}$kg (consistent with a two sigma error in the asteroid scattering determination; Hilton 1997 suggests possible systematic errors up to three sigma) and a corresponding density of $\rho = (1.79 \pm 0.95) \times 10^3 \mathrm{kg \cdot m^{-3}}$.

Our single albedo model would predict a lightcurve amplitude of $\Delta m = 0.08 \pm 0.05$ that is not consistent with the observed $\Delta m \approx 0.4$. That fact could be explained by the combined effect of the already mentioned underestimation of 15–Eunomia B diameter, the non sphericity, and the different albedo

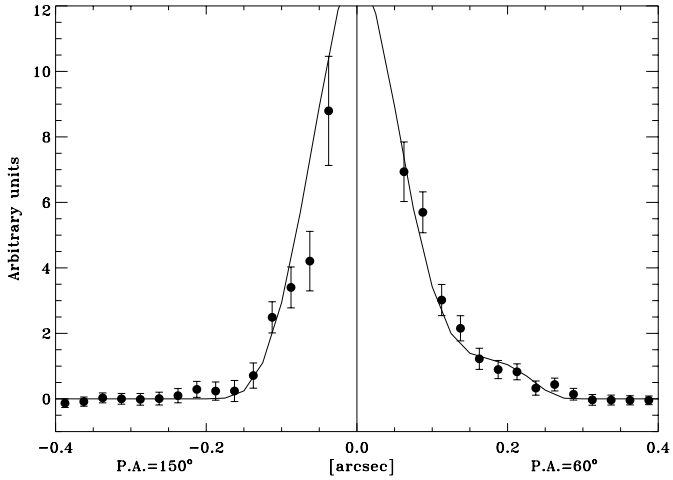

Fig. 6. The comparison of the ACF for the model described in the text with our measurements. On the right side the position angle is aligned with the two component model of 15–Eunomia; on the left side the position angle is orthogonal. Each experimental point is the average of a sector of an anulus with a width of $0.025'' \times 45^\circ$. The large error bars at small distances are related to the insufficient sampling of the corresponding anulus.

for the two components. It is very interesting to point out that the two sides of the ovoidal shaped model for 15–Eunomia exhibit different spectral behaviours (Reed et al. 1997).

Further constraints on our model can be placed by tidal stability considerations. A synchronous rotation should be achieved when the following relation, rearranged from Eq. (7) of van Flandern et al. (1979), holds:

$$\frac{P_{\mathrm{hours}}^{2/3} \cdot \rho_{\mathrm{kg \cdot m^{-3}}}^{1/3} \cdot D_A}{44.4 r} = 1. \qquad (6)$$

In our case the left–hand side of Eq. (6) amounts to 1.00 ± 0.34, well in agreement with a synchronous rotation. However, this configuration is unstable (Weidenschilling et al. 1989) and 15–Eunomia B should rapidly spiralize toward 15–Eunomia A. The observational upper limit on period variation (Magnusson 1986) determines a characteristic evolution time $t > 5.47 \times 10^{11}$ years: this is too large to be explained by any dynamic evolution model and the most likely scenario is that, if this is a double asteroid, 15–Eunomia A and B are already in contact as 216–Kleopatra (Storrs et al., 1999) 4179–Toutatis (Ostro et al. 1993) and 4769–Castalia (Ostro 1990). The estimations of the mass and the density would still be valid, because the system does not exchange angular momentum anymore and, in a certain sense, the orbital situation has been *frozen* at the contact's instant.

The final figures for the two proposed models of 15–Eunomia are reported in Table 3.

It is to be mentioned that adaptive optics observations of 15–Eunomia have been performed lately, confirming the elongated shape of this asteroid but excluding its duplicity (Dumas 1999).

4. Conclusions

Our results are somewhat encouraging from the instrumental point of view and, in our opinion, show that a program of direct size determination of a consistent ensemble of asteroids can be effectively carried out from a speckle facility aboard a 4m class telescope.

The measurements still depend upon some choice for the brightness distribution parameter. Full resolution of the asteroid surface is almost impossible with our facility. In addition, it is to be mentioned that we think that our data are too noisy to try to perform a reliable determination of k. Higher SNR specklegrams (obtainable with longer exposure time and better seeing conditions) could in principle be used to determine this coefficient in an independent way. Its effect on the estimated diameter of the asteroid can be retrieved by extensive numerical simulations: we found a nearly linear behaviour of the diameter estimate variation with the assumed k. A variation of $\Delta k = 0.1$ will cause a variation of the diameter of slightly less than 6%.

Speckle-based diameter measurements for asteroids depend even more on the assumptions about the geometrical parameters in those cases where inhomogeneities of the surface are present. It is however possible to calibrate our techniques using, for example, the asteroid 4 Vesta whose shape and albedo distribution are well known.

In our opinion, the corresponding uncertainties currently affecting our measurements do not undermine their usefulness, given that the mass determinations available to date are affected by errors which are not smaller than those affecting speckle observations. Further, this fact underlines the importance of performing these measures for a large number of objects, so that statistical conclusions can be drawn.

Finally, a few words should be added about the two models adopted for 15–Eunomia: the egg–shaped and the double contact binary.

Automatic and real–time data reduction does not help very much to solve the shape ambiguity, but it could be very useful to identify a number of suspect cases that can be further constrained by careful examination of the lightcurve and/or further observations with high angular resolution methods (HST, phase–resolving speckle or adaptive optics).

In fact, adaptive optics observations of asteroids have recently led to the discovery of a satellite of the asteroid 45–Eugenia (Merline 1999).

Acknowledgements. We thank the whole TNG commissioning team, led by F. Bortoletto, including C. Bonoli, A. Cavazza, L. Corcione, M. D'Alessandro, D. Fantinel, D. Gardiol, E. Giro, J.C. Guerra Ramon, D. Mancini, J.L. Medina, F. Paulli, C. Pernechele, P. Schipani, G. Tessicini, G. Trancho Lemes, C. Vuerli, A. Zacchei for their invaluable work. We thank C. Barbieri and F. Fusi Pecci for their continuous support during the realization of both the telescope and the adaptive optics instrument. Thanks are due to P. Farinella for some useful advices and to G. Valente for carefully reading of the manuscript. Thanks are also due to S. Mallucci, G. Baú and L. Traverso. This work has been funded by CRA and CNAA.

References

Albrecht R., Barbieri C., Adorf H.-M., et al., 1994, ApJ 435, L75
Angel J.R.P., 1977, Icarus 32, 450
Baier G., Weigelt G., 1983, A&A 121, 137
Barbieri C., 1997, SPIE 2871, 244
Barucci M.A., Cellino A., De Sanctis C., et al., 1992, A&A 266, 385
Baruffolo A., Ragazzoni R., Farinato J., 1998, SPIE 3353, 1138
Bortoletto F., Bonoli C., D'Alessandro M., et al., 1998, SPIE 3352, 91
Cellino A., Pannunzio R., Zappalá V., Farinella P., Paolicchi P., 1985, A&A 144, 355
Christou J.C., 1988, NOAO/ESO conf. on: High Resolution Imaging by Interferometry. 97
Drummond J.D., Cocke W.J., Hege E.K., Strittmatter P.A., Lambert J.V., 1985a, Icarus 61, 132
Drummond J.D., Hege E.K., Cocke W.J., et al., 1985b, Icarus 61, 232
Drummond J.D., Hege E.K., 1986, Icarus 67, 251
Drummond J.D., Eckart A., Hege E.K., 1988, Icarus 73, 1
Drummond J.D., Hege E.K., 1989, In: Binzel R.P., Gehrels T., Matthews M.S. (eds.) Asteroids II, University Arizona Press, Tucson, p. 171
Dumas C., 1999, private communication
Hapke B.W., 1984, Icarus 59, 41
Hilton J.L., Seidelmann P.K., Middour J., 1996, AJ 112, 2319
Hilton J.L., 1997, AJ 114, 402
Kuzmanoski M., Knezevic Z., 1993, Icarus 103, 93
Labeyrie A., 1970, A&A 6, 85
Magnusson P., 1986, Icarus 68, 1
Mallucci S., 1998, Tesi di Laurea in Astronomia, Universitá di Bologna
Marchetti E., Mallucci S., Ghedina A., et al., 1997, In: Barbieri C. (ed.) The Three Galileos: The Man, The Spacecraft, The Telescope. p. 383
McEwen A.S., 1991, Icarus 92, 298
Merline W.J., 1999, IAU Circ. 7129
Michalowski T., Velichko F.P., Lindgren M., et al., 1991, A&AS 91, 53
Minnaert M., 1941, ApJ 93, 403
Ostro S.J., Jurgens R.F., Rosema K.D., et al., 1993, BAAS 25, 1126
Ostro S.J., 1990, Astronomy 18, 38
Pehlemann E., Hofmann K.–H., Weigelt G., 1992, A&A 256, 701
Ragazzoni R., Bonaccini D., 1995, ESO conf. 54, 17
Ragazzoni R., Baruffolo A., Farinato J., et al., 1998, SPIE 3353, 132
Ragazzoni R., Baruffolo A., Marchetti E., et al., 2000, A&AS submitted
Reed K.L., Gaffey M.J., Lebofsky L.A., 1997, Icarus 125, 446
Roberts L.C. Jr., McAlister H.A., Hartkopf W.I., Franz O.G., 1995, AJ 110, 2463
Scaltriti F., Zappalá V., 1975, A&AS 19, 249
Scholl H., Schmadel L.D., Röser S., 1987, A&A 179, 311
Storrs A., Weiss B., Zellner B., et al., 1999, Icarus 137, 260
Tedesco E.F., 1989, In: Binzel R.P., Gehrels T., Matthews M.S. (eds.) Asteroids II, University Arizona Press, Tucson, p. 1090
Thiébaut E., 1994, A&A 284, 340
Tholen D.J., 1989, In: Binzel R.P., Gehrels T., Matthews M.S. (eds.) Asteroids II, University Arizona Press, Tucson, p. 1139
van Flandern T.C., Tedesco E.F., Binzel R.P., 1979, In: Gehrels T. (ed.) Asteroids. University of Arizona Press, Tucson, p. 443
Weidenschilling S.J., Paolicchi P., Zappalá V., 1989, In: Binzel R.P., Gehrels T., Matthews M.S. (eds.) Asteroids II, University Arizona Press, Tucson, p. 643
Williams J.G., 1989, In: Binzel R.P., Gehrels T., Matthews M.S. (eds.) Asteroids II, University Arizona Press, Tucson, p. 1034
Worden S.P., Stein M.K., Schmidt G.D., Angel J.R.P., 1977, Icarus 32, 450
Worden S.P., Stein M.K., 1979, AJ 84, 140